Spectroscopy 27 (2012) 35–48
DOI 10.3233/SPE-2012-0568
IOS Press

Spectroscopic (FT-IR, FT-Raman, ^{1}H and ^{13}C NMR) and theoretical studies of *p*-coumaric acid and alkali metal *p*-coumarates

Renata Świsłocka, Małgorzata Kowczyk-Sadowy, Monika Kalinowska and Włodzimierz Lewandowski *
Division of Chemistry, Bialystok University of Technology, Bialystok, Poland

Abstract. The evaluation of the electronic charge distribution in metal complexes enables more precise interpretation of mechanism by which particular metal ions affect biochemical properties of ligands [*J. Inorg. Biochem.* **99** (2005), 1407–1423, *J. Mol. Struct.* **919** (2009), 284–289]. In this paper we investigated the influence of alkali metal cations (lithium, sodium, potassium, rubidium and cesium) on the electronic structure of *p*-coumaric acid (*p*-CA). It allowed to observe the systematic changes in the spectra of investigated complexes depending on the position of the element in the periodic table. *p*-Coumaric acid is a derivative of cinnamic acid that occurs in several plant species. Li, Na, K, Rb and Cs *p*-coumarates were synthesized and the experimental and theoretical FT-IR, FT-Raman, ^{1}H and ^{13}C NMR spectra of *p*-coumaric acid and its salts were registered and analyzed. The structures, atomic charges, infrared and NMR spectra of *p*-coumaric acid and Li, Na, K salts were calculated by B3LYP/6-311++G** method.

Keywords: *p*-Coumaric acid, alkali metal *p*-coumarates, IR, Raman, NMR spectra

1. Introduction

Phenolic acids are compounds, which vary in their chemical structure and properties. *p*-Coumaric acid (3-hydroxycinnamic acid) is a natural phenolic acid existing in grapes and wine. In plants *p*-coumaric acid was found mainly in bound form, as a component of lignins and tannins in the form of esters and glycosides. In nature, cinnamic acid derivatives are important metabolic building blocks in the production of lignins for higher plants [6,11]. *p*-Coumaric acid belongs to a range of compounds that during degradation produces substances which due to their toxicity inhibit biological treatment of the effluents from the food processing industry [5]. *p*-Coumaric acid possesses antioxidant, antitumour and anti-inflammatory properties. This acid is an antioxidant which is implicated for the prevention of pathologies such as colon cancer and cardiovascular diseases. It has been reported that there is a high efficient intestinal absorption of *p*-coumaric acid *in vivo* [9].

The absorption and fluorescence behaviour of *p*-coumaric acid were investigated by Putschögl, Zirak and Penzkofer [10]. They noted, that acid exists in different ionic forms in aqueous solution depending on the pH. There is an equilibrium between the neutral form of *p*-coumaric acid (*p*-CA) and the single anionic form *p*-CA^{-} at low pH ($pK_{na} \approx 4.9$), and between the single anionic and the double anionic

*Corresponding author: Włodzimierz Lewandowski, Division of Chemistry, Bialystok University of Technology, Zamenhofa 29, 15-435 Bialystok, Poland. E-mail: w-lewando@wp.pl.

form p-CA^{2-} at high pH ($pK_{na} \approx 9.35$). The zinc complex of the p-coumaric acid was investigated by spectroscopic (FT-IR, UV-vis, X-ray) [1].

In this paper the influence of lithium, sodium, potassium, rubidium and cesium on the electronic system of the p-coumaric acid was studied. This paper presents spectroscopic vibrations (FT-IR, FT-Raman) and NMR (^{1}H and ^{13}C) study of the series of alkali metal coumarates from lithium to cesium p-coumarates. This data were not yet presented and discussed in the literature. Characteristic shifts of band wavenumbers and changes in band intensities from the FT-IR, FT-Raman and NMR spectra along the metal series (Li → Cs) were observed. Optimized geometrical structures, atomic charges, infrared and NMR spectra of p-coumaric acid and Li, Na and p-coumarates were calculated by B3LYP/6-311++G** method. The relationship between certain parameters of the alkali metal ions and electronic charge distribution in the whole molecule of the studied compounds was discussed. We investigated correlation between molecular structure and macroscopic properties of alkali metal salts of p-coumaric acid. In this way it may become possible to find compounds with specific biological activity not by a process of trial and error, but on the basis of strictly described dependencies between the structure and biological activity of compounds.

2. Experimental section

Lithium, sodium, potassium, rubidium and cesium p-coumarates were prepared by dissolving the powder of p-coumaric acid in a water solution of the appropriate metal hydroxide in a stoichiometric ratio of 1:1. All reagents were Aldrich analytical chemicals.

The IR spectra were recorded with the Equinox 55 Bruker FT-IR spectrometer within the range of 4000–400 cm^{-1}. The resolution of spectrometer was 1 cm^{-1}. Samples in the solid state were measured in KBr matrix. Weighted ratio of potassium bromide to the test substance was 100:1. The pellets were obtained with hydraulic press under 739 MPa pressure. Raman spectra of solid samples in capillary tubes were recorded in the range of 4000–100 cm^{-1} with a FT-Raman accessory of the Perkin-Elmer system 2000. The NMR spectra of DMSO solution were recorded with a Bruker AC 200F unit at room temperature. Tetramethylsilane (TMS) was used as an internal references. Crystal structure of p-coumaric acid was found in crystallographic database CSD (Crystallographic Structural Data Base) and visualized with the Mercury 1.4.2 program [3,15]. To calculate optimized geometrical structures of studied compounds, a density functional theory in B3LYP/6-311++G** level was used [4]. The geometric aromaticity indices [7] were calculated.

3. Results and discussion

3.1. Calculated geometrical structure

The distances between atoms in p-coumaric acid and Li, Na, K coumarates and the angles between bonds were calculated and presented in Table 1. The atoms numbering is shown in Fig. 1. Substitution of metal cation in a place of carboxylic group hydrogen of p-coumaric acid does not cause significant changes in the electronic charge distribution of the ring, but it mainly affects the parameters of double bond –C=C–. One may see a regular decrease or increase in the bond lengths in the order: Li → Na → K p-coumarates, i.e. distances C1–C9, C7–C8, C4–O3 increase and C8–C9, C7–O1, C7–O2 decreases in

Table 1
Values of distances (Å) between atoms, bond angles (°), geometric aromaticity indices, dipole moments and energies calculated for *p*-coumaric acid and lithium, sodium and potassium *p*-coumarates

	Acid			Li	Na	K
	Calculated	Experimental [15]	Experimental [3]			
Distances						
C1–C2[a]	1.407	1.410	1.382	1.406	1.406	1.406
C2–C3	1.387	1.391	1.387	1.388	1.389	1.389
C3–C4	1.396	1.396	1.377	1.395	1.394	1.394
C4–C5	1.400	1.398	1.382	1.399	1.398	1.398
C5–C6	1.386	1.392	1.383	1.387	1.388	1.388
C6–C1	1.406	1.403	1.396	1.405	1.405	1.405
C1–C9	1.459	1.468	1.469	1.462	1.464	1.465
C7–C8	1.466	1.479	1.471	1.480	1.491	1.496
C8–C9	1.346	1.349	1.323	1.343	1.341	1.341
C4–O3	1.363	1.373	1.381	1.367	1.369	1.370
C7–O1	1.364	1.272	1.257	1.277	1.272	1.270
C7–O2	1.213	1.275	1.275	1.277	1.273	1.271
O1–H1(M)	0.968	–	–	1.850	2.204	2.511
O3–H4	0.963	–	1.091	0.963	0.963	0.963
C2–H2	1.085	–	0.974	1.085	1.085	1.085
C3–H3	1.083	–	0.910	1.083	1.083	1.083
C5–H5	1.086	–	0.999	1.086	1.087	1.087
C6–H6	1.083	–	0.986	1.083	1.083	1.083
C9–H8	1.086	–	0.930	1.087	1.087	1.088
C8–H7	1.083	–	0.936	1.084	1.084	1.085
O2–Me	–	–	–	1.854	2.206	2.515
Angles						
C1–C2–C3	121.821	121.270	121.640	121.915	121.993	122.035
C2–C3–C4	119.495	118.970	118.670	119.516	119.523	119.526
C3–C4–C5	119.870	121.230	121.410	119.801	119.746	119.720
C4–C5–C6	119.870	118.930	119.010	120.073	120.108	120.128
C5–C6–C1	121.207	121.420	121.030	121.300	121.352	121.377
C6–C1–C2	117.559	118.180	118.230	117.396	117.278	117.214
C2–C1–C9	118.973	118.300	119.340	119.132	119.197	119.235
C1–C9–C8	127.487	126.120	127.770	127.911	127.866	127.913
C7–C8–C9	124.001	120.750	122.560	121.938	122.377	122.518
C8–C7–O1	114.152	–	–	120.972	119.750	119.403
C8–C7–O2	124.269	–	–	118.415	117.007	116.665
C7–C8–H7	113.231	–	–	114.956	114.849	114.819
C9–C8–H7	122.768	–	–	123.107	122.774	122.662
C8–C9–H8	117.238	–	–	116.214	116.200	116.131
C1–C9–H8	115.275	–	–	115.875	115.934	115.956
C9–C1–C2	118.973	–	–	119.132	119.197	119.235
C1–C2–H2	119.080	–	–	118.977	118.926	118.892
C3–C2–H2	119.100	–	–	119.108	119.081	119.073
C3–C4–O3	117.524	–	–	117.624	117.699	117.734

Table 1
(Continued)

	Acid			Li	Na	K
	Calculated	Experimental [15]	Experimental [3]			
C4–C5–H5	119.951	–	–	119.938	119.919	119.909
C6–C5–H5	120.000	–	–	119.989	119.973	119.963
C5–C6–H6	118.679	–	–	118.752	118.757	118.770
C1–C6–H6	120.114	–	–	119.948	119.892	119.853
C6–C1–C9	123.468	–	–	123.471	123.525	123.551
C9–C8–C7	124.001	–	–	121.938	122.377	122.518
C5–C4–O3	122.605	–	–	122.575	122.555	122.546
C4–O3–H4	110.106	–	–	109.880	109.723	109.632
C7–O1–H1(M)	106.369	–	–	82.960	87.944	91.651
O1–C7–O2	114.152	123.880	123.770	120.613	123.243	123.932
C7–O2–M	–	–	–	82.810	87.802	91.423
O1–M–O2	–	–	–	73.617	61.011	52.994
C1–C9–C8–C7	−179.993	179.040	178.610	180.000	179.997	179.991
C6–C1–C9–C8	0.064	1.550	2.160	−0.089	−0.126	−0.162
C9–C8–C7–O2	179.989	2.300	2.270	−179.995	−179.989	−179.979
C9–C8–C7–O1	−0.016	177.400	177.700	0.004	0.011	0.025
Geometric aromaticity indices						
Aj	0.992	0.995	0.996	0.994	0.994	0.995
BAC	0.887	0.916	0.921	0.900	0.907	0.910
HOMA	0.963	0.961	0.988	0.966	0.968	0.969
GEO	0.017	0.011	0.009	0.014	0.013	0.012
EN	0.020	0.028	0.003	0.019	0.019	0.019
I_6	93.134	94.523	95.108	93.767	94.091	94.231
Dipole moment						
Debye (D)[b]	3.340	–	–	2.192	5.243	7.034
Energy						
Hartree[c]	−573.619			−580.617	−735.378	−1173.022

[a]Atom numbering; [b]1 D = 1.33654×10^{-30} C × m; [c]1 Hartree = 2625.5 kJ/mol.

the series. The rest of bond lengths do not change in a significant way. Among the calculated angles the following ones: C7–O1–H1(M), O1–C7–O2, C7–O2-M, O1-M–O2 change their values significantly.

The geometric aromaticity indices: Aj – normalized function of the bond variance lengths; BAC – bond alternation coefficient; HOMA – harmonic oscillator model of aromaticity and I_6 – Bird's index [7] were calculated and obtained results were presented in Table 1. The values of Aj (0.992–0.995) and HOMA (0.963–0.969) aromaticity indices are almost the same in the series: acid → Li → Na → K. Little differences are observed for BAC (0.887–0.910) and the highest values are obtained in the case of Bird's indices. The calculated indices show a slightly increase in the aromaticity of studied molecules in the series: acid → Li → Na → K salts.

Dipole moments and energies for *p*-coumarates were calculated (Table 1). Comparing values of dipole moment for molecules of lithium, sodium and potassium salts of *p*-coumaric acid an increasing tendency along the series: lithium (2.192 D) → sodium (5.243 D) → potassium (7.034 D) *p*-coumarates is observed. Such a value for free acid (3.340 D) is located between values for lithium and sodium *p*-

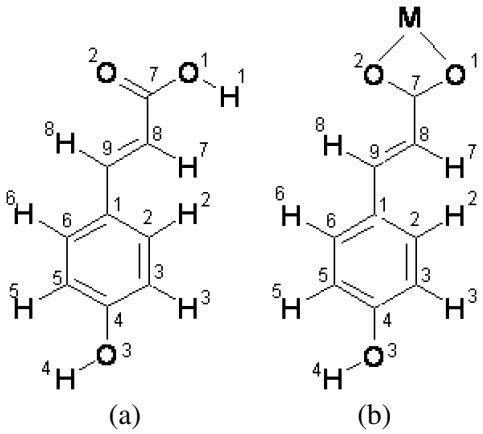

Fig. 1. Structures of (a) p-coumaric acid and (b) alkali metal (M) p-coumarate.

coumarates. The values of energy decrease from acid to potassium salt. This indicates that the stability of the studied molecules increases in this order what confirms the values of aromaticity indices calculated for studied compounds.

The Mulliken and APT atomic charges on the atoms in lithium, sodium and potassium p-coumarates are gathered in Table 2. The calculated atomic charges implicated a decrease in the electron density around: C1, C3, C6, C7, C9 atoms (Mulliken) and C1, C3, C5, C8 atoms (APT), an increase around C2, C4, C5, C8 atoms (Mulliken) and C2, C4, C6, C7, C9 atoms (APT) in the salt molecules comparing to the acid molecule. The negative charge gathered on O1 and O2 atoms regularly increases in series: lithium $\rightarrow$ sodium $\rightarrow$ potassium p-coumarates. The values of atomic charges around the aromatic ring carbon atoms of ligand change in following series q(C1) $<$ q(C2) $<$ q(C5) $<$ q(C3) $<$ q(C4) $<$ q(C6). The total electron density in the carboxylic group increases along with the series Li $\rightarrow$ Na $\rightarrow$ K coumarates.

3.2. FT-IR and FT-Raman spectra

The wavenumbers, intensities and assignments of the bands occurring in the FT-IR and FT-Raman spectra of p-coumaric acid and alkali metal coumarates are presented in Table 3. The bands are numbered along with the notation used by Varsányi [16]. The assignment was done on the basis of literature data [10] and calculations performed in the frame of this paper. The symbol "ν" denotes stretching vibrations, "β" denotes in-plane deformations, "γ" denotes out-of-plane deformations; "ϕ(CCC)" denotes the aromatic ring out-of-plane deformations and "α(CCC)" denotes the aromatic ring in-plane deformations. In addition, the band is marked with "*as*" – asymmetric vibrations, "*s*" – symmetric, "*ar*" – vibrations of the aromatic ring. The calculated wavenumbers of IR spectra of p-coumaric acid, lithium, sodium and potassium coumarates was obtained by B3LYP/6-311++G** method (Tables 3 and 4). The experimental and calculated spectra of p-coumaric acid are presented in Fig. 2. Correlation between calculated and experimentally obtained wavenumbers of the IR spectra of p-coumaric acid and Li, Na, K coumarates are follows: 0.995 (p-coumaric acid) (Fig. 3), 0.987 (Li p-coumarate), 0.990 (Na p-coumarate), 0.993 (K p-coumarate). The obtained correlation coefficients show good agreement between experimental and theoretical data.

The O–H group gives rise to three vibrations (stretching, in-plane bending and out-of-plane bending vibrations). In our case a very strong band at 3383 cm^{-1} (IR_{exp}) is assigned to $(OH)_{ar}$. stretching vibrations. The O–H in-plane bending vibration in the phenols, in general can be found in the region

Table 2
The atomic charges for *p*-coumaric acid as well as for lithium, sodium and potassium *p*-coumarates calculated in the B3LYP/6-311++G6** level

Atom position	*p*-Coumaric acid		Li *p*-coumarate		Na *p*-coumarate		K *p*-coumarate	
	Mulliken	APT	Mulliken	APT	Mulliken	APT	Mulliken	APT
C1	1.315	−0.307	1.441	−0.223	1.455	−0.161	1.450	−0.127
C2	0.342	0.145	0.229	0.108	0.249	0.083	0.226	0.070
C3	−0.319	−0.207	−0.210	−0.187	−0.222	−0.174	−0.227	−0.166
C4	−0.481	0.753	−0.545	0.718	−0.569	0.695	−0.526	0.683
C5	−0.199	−0.246	−0.200	−0.220	−0.158	−0.206	−0.181	−0.199
C6	−1.263	0.105	−1.227	0.074	−1.309	0.054	−1.255	0.044
C7	0.035	1.591	0.157	1.542	0.320	1.472	0.342	1.485
C8	−0.093	−0.575	−0.155	−0.513	−0.179	−0.425	−0.164	−0.400
C9	−0.252	0.471	−0.090	0.359	−0.051	0.269	−0.139	0.222
H1 (Me)	0.290	0.304	0.189	0.849	0.485	0.869	0.993	0.961
H2	0.166	0.047	0.160	0.044	0.159	0.042	0.155	0.041
H3	0.191	0.058	0.188	0.053	0.185	0.049	0.183	0.048
H4	0.271	0.301	0.263	0.295	0.262	0.292	0.262	0.290
H5	0.160	0.027	0.151	0.022	0.151	0.019	0.147	0.017
H6	0.072	0.049	0.083	0.048	0.074	0.048	0.076	0.047
H7	0.204	0.048	0.146	0.036	0.158	0.028	0.156	0.024
H8	0.190	0.058	0.174	0.057	0.174	0.057	0.172	0.056
O1	−0.209	−0.776	−0.359	−1.034	−0.491	−1.054	−0.532	−1.079
O2	−0.296	−0.967	−0.340	−1.111	−0.462	−1.135	−0.503	−1.152
O3	−0.225	−0.881	−0.229	−0.872	−0.233	−0.866	−0.237	−0.864
Sum: Ring	−0.605	0.243	−0.562	0.270	−0.554	0.291	−0.513	0.305
C=C	−0.345	−0.104	−0.245	−0.154	−0.230	−0.156	−0.303	−0.178
COO^-	−0.470	−0.152	−0.542	−0.647	−0.633	−0.673	−0.693	−0.746

1150–1250 cm^{-1} and is not much affected due to hydrogen bonding unlike to stretching and out-of-plane bending wavenumbers [13,14]. The O–H out-of-plane bending mode for the free molecule lays below 300 cm^{-1} and it is beyond the infrared spectral range of the present investigation. However, for the associated molecule the O–H out-of-plane bending mode lies in the region 517–710 cm^{-1} in both intermolecular and intramolecular associations, the wavenumber is at a higher value than in free O–H [16]. In our present investigation a strong band observed in spectrum at 557 cm^{-1} (IR_{exp}), 552 cm^{-1} (R_{exp}), is assigned to O–H out-of-plane bending vibrations.

In the 3800–2950 cm^{-1} (IR_{exp}) and 3072–3007 cm^{-1} (R_{exp}) spectra region some of the major absorption bands are due to the C–H stretches (aromatic and aliphatic). Replacement of the carboxylic group hydrogen with a metal ion brought about characteristic changes in the IR and Raman spectra of the metal *p*-coumarates in comparison with the spectra of ligand [12]. One can observe disappearance of bands of the symmetric and asymmetric valence vibrations: stretching ν(C=O) at 1672 (IR) cm^{-1}, β(C=O) at 692 (IR) and 680 cm^{-1} (Raman), as well as γ(C=O) at 557 (IR) and 552 cm^{-1} (Raman) of the carbonyl group; disappearance of stretching vibrations ν(O–H) at 2839 cm^{-1} (IR) and deformation vibrations β(O–H); appearance of bands of the asymmetric and symmetric vibrations of the carboxylate anion $\nu_{as}(COO^-)$, $\nu_s(COO^-)$, as well as $\beta_{as}(COO^-)$, $\beta_s(COO^-)$, and disappearance or changes in positions and intensities of some aromatic bands.

Table 3
The wavenumbers (cm^{-1}) and assignments of bands occurring in the experimental FT-IR, FT-Raman and calculated FT-IR spectra of *p*-coumaric acid

p-Coumaric acid				Assignment	No. [16]
IR_{exp}	R_{exp}	IR_{calc}	Int.		
3383 s		3830	100.35	$\nu(OH)_{ar}$	
		3779	111.72	$\nu(OH)$	
		3198	4.32	$\nu(CH)_{ar}$	2
3080 w	3069 w	3196	7.20	$\nu(CH)_{ar} + \nu(CH)_{C=C}$	20a
3026 w	3025 vw	3186	2.26	$\nu(CH)_{ar} + \nu(CH)_{C=C}$	20b
2963 w		3171	5.92	$\nu(CH)_{ar} + \nu(CH)_{C=C}$	7b
		3162	0.56	$\nu(CH)_{ar} + \nu(CH)_{C=C}$	
		3154	16.95	$\nu(CH)_{ar}$	
2839–2513 m				$\nu(OH)_{ar}$	
1672 vs		1770	702.90	$\nu(C{=}O)$	
1628 s	1636 m	1676	29.95	$\nu(CC)_{C=C}$	
1601 vs	1606 vs	1644	332.46	$\nu(CC)_{ar}$	8a
1591 s	1593 m	1619	8.36	$\nu(CC)_{ar}$	8b
1512 s	1519 w	1544	80.38	$\nu(CC)_{ar}$	19a
1449 vs	1448 w	1465	76.96	$\nu(CC)_{ar}$	19b
1422 m		1372	122.23	$\beta(CH)_{C=C}$	
1379 m		1368	3.27	$\beta(CH)_{C=C} + \beta(OH)_{ar}$	14
1327 s		1352	41.75	$\beta(CH)_{C=C}$	
1314 s	1306 w	1296	5.61	$\beta(CH)_{C=C} + \beta(CH)_{ar}$	3
1283 m	1282 w	1172	604.27	$\nu(C{-}OH)$	
1244 vs	1260 m	1192	66.26	$\beta(OH)_{ar}$	
1215 vs	1213 m	1238	22.05	$\beta(CH)$	13
1173 s	1172 s	1197	3.83	$\beta(CH)_{ar}$	9a
1105 m		1125	73.15	$\beta(CH)$	18b
1013 w		1024	0.20	$\beta(CH)$	18a
		1018	34.34	$\gamma(CH)_{C=C}$	
978 s	977 w	911	28.94	$\nu(CCO)$	
941 m	952 vw	969	0.71	$\gamma(CH)_{ar}$	17a
		939	0.31	$\gamma(CH)_{ar}$	5
		892	7.85	$\gamma(CH)_{C=C}$	
920 m		751	3.38	$\gamma(CO)$	
860 w	864 w	811	11.59	$\gamma(CH)$	10a
833 s	837 w	843	67.23	$\gamma(CH)_{ar}$	17b
799 m	800 w	871	3.82	$\alpha(CCC)$	1
692 m	680 vw	633	33.31	$\beta(CO)$	
646 w	645 vw	700	3.17	$\phi(CC)$	4
		656	0.77	$\alpha(CCC)$	6b
557 m	552 vw	540	123.52	γOH	
525 m	534 vw	514	31.82	$\alpha(C{=}C{-}C)$	
517 m	516 vw	513	2.27	$\phi(CC)$	16b
453 w		418	0.92	$\phi(CC)$	16a
430 vw	421 vw	417	5.62	$\beta(CH)$	9b
		329	93.43	$\gamma(OH)_{ar}$	

Notes: s – strong; vs – very strong; m – medium; sh – shoulder; w – weak; vw – very weak.

Table 4

The wavenumbers (cm^{-1}) and assignments of bands from the IR (experimental and theoretical) and Raman (experimental) spectra of lithium, sodium, potassium, rubidium and cesium *p*-coumarates

Li *p*-coumarate			Na *p*-coumarate			K *p*-coumarate			Rb *p*-coumarate		Cs *p*-coumarate		Assignments	No. [16]
IR_{exp}	R_{exp}	IR_{calc}	IR_{exp}	R_{exp}	IR_{calc}	IR_{exp}	R_{exp}	IR_{calc}	IR_{exp}	R_{exp}	IR_{exp}	R_{exp}		
3412 m	–	3833	3422 s	–	3834	3426 m	–	3835	3422 m	–	–	–	$\nu(OH)_{ar}$	
-	–	3189	3375 s	–	3193	–	–	–	3374 m	–	–	–	$\nu(CH)_{ar}$	2
3358 m	–	–	–	–	–	3356 m	–	–	–	–	3358 w	–	$\nu(CH)_{ar}$	
3071 w	3072 w	3149	3076 m	3079 w	3188	3076 vw	3076 vw	3192	3078 w	3064 vw	3071 w	3058 vw	$\nu(CH)_{ar} + \nu(CH)_{C=C}$	20a
3028 w	3047 w	–	3030 m	3042 w	3174	3030 m	3043 vw	3146	3030 w	3043 vw	3032 vw	–	$\nu(CH)_{ar} + \nu(CH)_{C=C}$	20b
2962 vw	–	–	2950 vw	–	3168	–	–	–	–	–	2963 vw	–	$\nu(CH)_{ar} + \nu(CH)_{C=C}$	7b
2812 w	–	–	2810 w		–	2808 w	–	–	2810 w	–	2810 m	–	$\nu(OH)_{ar}$	
1640 s	1640 vs	1685	1638 s	1642 vs	1686	1638 s	1635 s	1687	1640 s	1636 s	1635 s	1636 w	$\nu(CC)_{C=C}$	
1606 s	1612 vs	1647	1609 s	1614 s	1647	1611 s	1609 vs	1678	1611 s	1609 vs	1607 m	1610 s	$\nu(CC)_{ar}$	8a
1595 s	–	1621	1597 s	1596 w	1621	1595 m	1587 s	1622	1597 m	1586 m	1595 s	1593 m	$\nu(CC)_{ar}$	8b
1574 vs	1574 vw	1525	1549 vs	1538 w	1548	1555 vs	1554 w	1558	1549 vs	1557 vw	1555 s	1556 w	$\nu_{as}(COO^-)$	
1512 s	1517 w	1544	1514 vs	1519 w	1541	1514 s	1520 vw	1541	1515 s	1520 vw	1510 vs	1519 vw	$\nu(CC)_{ar}$	19a
1450 m	1448 w	1464	1449 s	1450 w	1461	1447 s	1457 vw	1461	1448 s	1460 vw	–	–	$\nu(CC)_{ar}$	19b
1418 vs	1424 w	1430	1414 vs	1424 w	1406	1416 vs	–	1400	1414 vs	1415 w	1402 m	1405 vw	$\nu_s(COO^-)$	
1385 s	–	1366	1389 sh	1388 w	1364	1387 s	1390 vw	1364	1379 s	1385 w	1368 vs	1366 w	$\beta(CH)_{C=C} + \beta(OH)_{ar}$	14
1315 w	1317 vw	1320	1312 w	1312 w	1318	1314 m	1314 vw	1316	1312 m	1313 vw	–	1315 w	$\beta(CH)_{C=C} + \beta(CH)_{ar}$	3
1290 w	1292 w	–	1292 s	1294 w	–	1290 m	1283 w	–	1292 m	1291 w	1292 m	1294 vw	$\beta(CH)_{C=C}$	
1256sh	–	1225	1258 vs	–	1223	1261 s	–	1221	1258 s	–	1273 s	1274 w	$\beta(CH)_{C=C}$	
1244 s	1251 s	–	1244 vs	1248 s	–	1244 s	1223 s	–	1244 s	1248 s	1236 s	1235 vs	$\beta(OH)_{ar}$	
1173 m	1174 m	1195	1173 s	1176 m	1194	1173 m	1172 m	1194	1173 m	1171 m	1167 m	1169 m	$\beta(CH)_{ar}$	9a
–	–	1187	–	–	1187	–	–	1187	–	–	–	–	$\beta(OH)_{ar}$	
1103 m	1105 vw	1123	1103 s	1079 vw	1122	1103 m	–	1121	1103 m	1104 vw	1103 w	1106 vw	$\beta(CH)$	18b
1015 w	–	1025	1015 w	–	1026	1013 w	–	1026	1015 w	1013 vw	1013 w	–	$\beta(CH)$	18a
–	–	1023		–	1022	–	–	1021			–	–	$\gamma(CH)_{C=C}$	
982 s	981 w	989	970 s	969 w	983	970 s	973 vw	975	968 s	974 w	986 m	986 vw	$\nu(CCO)$	
939 w	–	969	941 w	–	967	939 w	–	–	941 vw	–	949 w	–	$\gamma(CH)_{ar}$	17a
887 m	892 w	–	878 m	879 w	941	880 w	–	–	880 m	–	878 w	880 w	$\gamma(CH)_{ar}$	5
864 w	866 w	815	–	865 w	810	868 vw	866 w	–	–	866 w	860 w	862 w	$\gamma(CH)$	10a
839 s	821 vw	845	835 vs	832 w	844	833 s	823 vw	843	833 s	830 vw	833 m	–	$\gamma(CH)_{ar}$	17b
800 m	802 w		799 m	802 w	872	799 m	808 w	–	799 m	808 w	800 m	807 w	$\alpha(CCC)$	1
717 m	716 vw	756	718 s	716 w		718 m	707 vw	726	718 m	716 vw	710 m	705 vw	$\gamma_s(COO^-)$	
643 sh	644 vw	706	644 m	645 w	705	644 vw	645 w	704	642 m	645 w	644 m	647 w	$\phi(CC)$	4
563 m	–	617	542 s	542 vw	656	542 m	546 w	–	542 m	553 vw	552 m	553 vw	$\alpha(CCC)$	6b
534 m	521 vw	–	530 s	530 vw	530	529 m		–	530 m	525 vw	529 m	530 vw	$\beta_{as}(COO^-)$	
527 sh	–	–	511 s	511 vw	519	511 m		–	511 m	–	515 m	–	$\phi(CC)$	16b
461 w	–	–	–	–	–	457 w	460 vw	–	–	461 vw	455 w	460 vw	$\phi(CC)$	16a
432 m	–	–	–	–		–	–	–	422 w	–	415 w	418 vw	$\beta(CH)$	9b

Notes: s – strong; vs – very strong; m – medium; sh – shoulder; w – weak; vw – very weak.

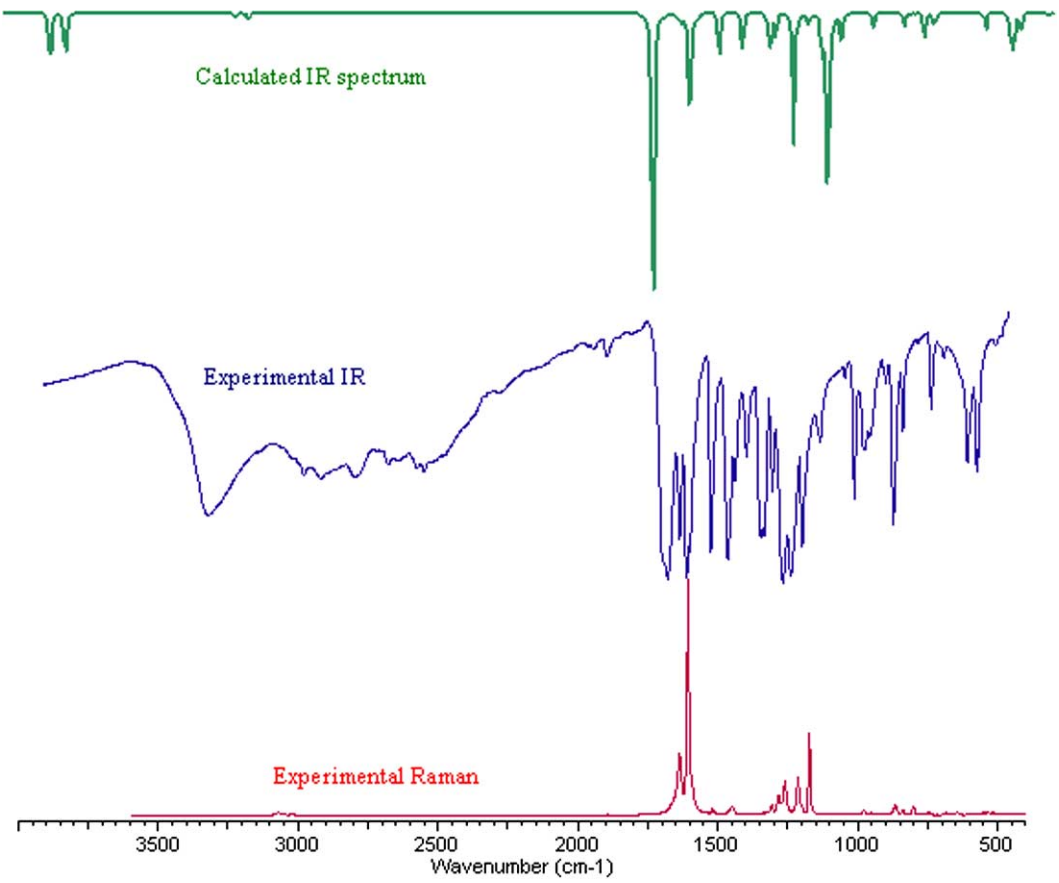

Fig. 2. Experimental Raman, IR and calculated IR spectra of *p*-coumaric acid. (Colors are visible in the online version of the article; http://dx.doi.org/10.3233/SPE-2012-0568.)

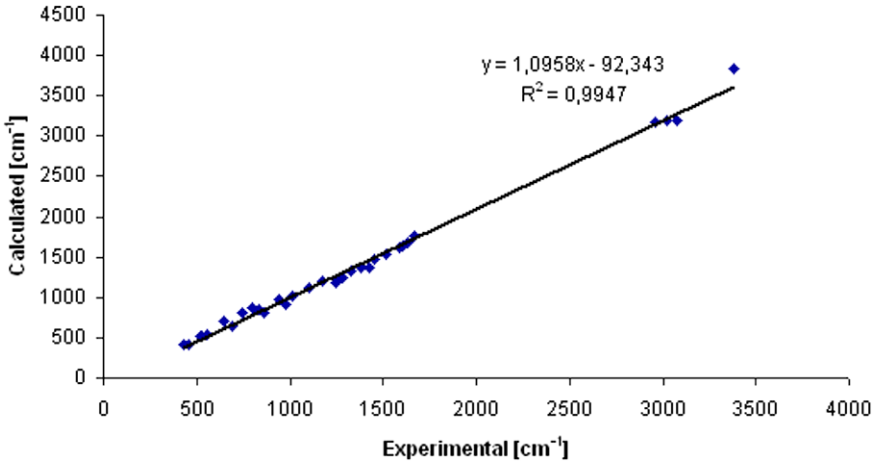

Fig. 3. Correlation between calculated and experimentally obtained wavenumbers from the IR spectra of *p*-coumaric acid. (Colors are visible in the online version of the article; http://dx.doi.org/10.3233/SPE-2012-0568.)

Bands originating from carboxylate anion vibrations are: (1) asymmetric stretches $\nu_{as}(COO^-)$, located at 1533, 1538, 1554 and 1557 cm^{-1} for Li, Na, K and Rb *p*-coumarates, respectively; (2) symmetric stretches $\nu_s(COO^-)$, at 1424, 1424 and 1415 cm^{-1} for Li, Na, K and Rb *p*-coumarates, respectively; (3) in-plane asymmetric deformations $\beta_{as}(COO^-)$ at 521, 530, 525 and 530 cm^{-1} for Li, Na, Rb and Cs *p*-coumarates, respectively; (4) out-of-plane symmetric deformations $\gamma_s(COO^-)$ at 716, 716, 707 and 716 cm^{-1} for Li, Na, K and Rb *p*-coumarates, respectively. There is an increase in the difference between wavenumbers of asymmetric and symmetric stretches of the carboxylic anion vibrations $\Delta\nu(COO^-)$ spectra along the series Na → K → Rb → Cs *p*-coumarates, i.e. 135, 139, 142 and 178 cm^{-1}, respectively. For Li *p*-coumarate the $\Delta\nu(COO^-)$ amounts to 156 cm^{-1}. Only in the theoretical spectra there is an explicit increase in the value of $\Delta\nu(COO^-)$ in the series Li → Na → K, i.e. 95, 142 and 158 cm^{-1}. It may mean different type of coordination in case of lithium salt and the rest of *p*-coumarates. During calculations the same type of metal coordination in case of Li, Na and K salt was assumed.

In the IR spectrum of *p*-coumaric acid, there are four main aromatic bands $\nu(CC)_{ar}$ that are located at 1601, 1591, 1512 and 1449 cm^{-1} i.e. 8a, 8b, 19a and 19b. In the case of metal *p*-coumarates these bands are locate in the range of 1611–1447 cm^{-1}. The $\nu(CC)_{ar}$ bands that occur in the IR spectra of *p*-coumarates have similar intensity as compared to those in the IR spectra of *p*-coumaric acid.

The bands of the β(CH) vibrations are located in the range 1422–1013 cm^{-1} (IR) and 1390–1013 cm^{-1} (Raman). The β(CH) bands that occur in the IR spectra of salts have similar intensity as compared to those in the IR spectra of *p*-coumaric acid. The bands no. 13 are present only in the spectra of ligand. The bands of the γ(CH) vibrations are located in the range 949–833 cm^{-1} (IR) and 952–923 cm^{-1} (Raman). There is a lack of band no. 5 in the spectra of acid. The bands of the ϕ(CC) vibrations are located in the range 646–453 cm^{-1} (IR) and 647–460 cm^{-1} (Raman). Only band no. 16a is located at higher wavenumber in the IR spectra of *p*-coumarates than in the spectra of ligand. Other bands no. 4 and 16b (except Na coumarate) are shifted towards lower wavenumber in the spectra of metal compounds compared with the spectra of *p*-coumaric acid. The bands of the α(CCC) vibrations are located in the range 800–525 cm^{-1} (IR) and 807–542 cm^{-1} (Raman). Most of this bands in the spectra of metal compounds are shifted to higher wavenumbers compared to ligand. The wavenumbers of band no. 6b increase along the series: Na → K → Rb → Cs (Raman).

Comparing spectroscopic results obtained for alkali metal *p*-coumarates to the respectively values of *p*-coumaric acid, certain changes of intensities and wavenumbers of the bands of aromatic system occur. The wavenumbers of bands numbered as 3, 7b, 14, 16b and 20a decrease in IR and Raman spectra of salts in comparison to free acid. The rest of bands are located at higher wavenumbers in the spectrum of *p*-coumarates.

3.3. NMR spectra

^{1}H NMR and ^{13}C NMR spectra of lithium, sodium, potassium, rubidium and cesium *p*-coumarates were recorded. Theoretical (B3LYP/6-311++G**) and experimental chemical shifts from the NMR spectra of *p*-coumarates in comparison to *p*-coumaric acid are gathered in Tables 5 and 6.

The chemical shifts of protons (^{1}H NMR) and carbons (^{13}C NMR) in the series of alkali metal coumarates express the influence of studied metal cations on the electronic charge distribution around carbon and hydrogen atoms [12]. One may observe a decrease in chemical shifts in case of all protons in comparison to appropriate shifts in the spectra of ligand (Fig. 4). It points at an increase in the screening of aromatic protons as a consequence of the circular current weakening, and it is an evidence that

Table 5
Experimental chemical shifts of p-coumarates in ^{1}H and ^{13}C NMR spectra, δ (ppm); atom numbering in Fig. 1

	p-Coumaric acid	Li p-coumarate	Na p-coumarate	K p-coumarate	Rb p-coumarate	Cs p-coumarate
Proton number						
1	12.13	–	–	–	–	–
2 and 6	7.49	7.22	7.13	7.10	7.02	7.02
3 and 5	6.79	6.77	6.75	6.76	6.73	6.71
4	9.96	10.12	–	–	–	–
7	6.29	6.30	6.20	6.18	6.12	6.11
8	7.52	7.28	7.26	7.23	7.21	7.19
Carbon number						
1	125.36	126.42	126.39	126.46	126.01	127.19
2 and 6	130.17	128.40	128.40	128.65	128.15	128.16
3 and 5	115.83	115.84	115.87	115.90	115.96	116.13
4	159.67	159.14	159.18	159.08	159.72	160.66
7	168.05	171.83	171.84	172.14	170.61	170.64
8	115.41	124.97	124.96	124.31	125.88	125.51
9	144.27	135.95	136.95	138.06	135.97	136.19

alkali metals perturb the electronic charge distribution in the molecule. Moreover, the chemical shifts of particular protons decrease in the following series: Li → Na → K → Rb → Cs, what suggest that destabilisation of the electronic system increase in the same order.

In the ^{13}C NMR spectra of p-coumarates there is no regularity in the chemical shifts of carbons along the series of alkali metal p-coumarates. The signals from carbons no. 2, 6, 9 and 4 (except Rb and Cs coumarate) are shifted upfield in comparison to the appropriate signals in the spectrum of ligand, whereas the signals from carbons no. 1, 3, 5, 7 and 8 are shifted up field (Fig. 5). This indicate the decrease in the electron density around carbons no. 1, 3, 5, 7 and 8, and an increase in the electron charge density in case of remaining carbon atoms.

The linear correlation between calculated and experimental data of ^{13}C NMR is noted. The data show a good correlation between predicted and observed carbon chemical shifts. The correlation coefficients between theoretical and experimental ^{13}C NMR shifts for p-coumaric acid, lithium, sodium and potassium salts are amount to 0.975, 0.943, 0.945 and 0.949, respectively. The lower correlation coefficients were obtained for the linear correlation between calculated and experimental date of ^{1}H NMR.

The calculated APT atomic charges in a very good manner reflect the changes in the electronic charge density described by experimental NMR spectra. According to calculated atomic charges a decrease in the electron density around: C1, C3, C5, C8 atoms (APT), an increase around C2, C4, C6, C7, C9 atoms (APT) is observed in the salt molecules comparing to the acid molecule. The relationship between experimental chemical shifts from the ^{13}C NMR spectra and calculated atomic charges for p-coumaric acid and p-coumarates was done. The highest correlation coefficients were obtained for the linear correlation between the chemical shifts the APT (for p-coumaric acid: 0.913; for Li salt: 0.883; for Na salt: 0.901; for K salt: 0.909). Whereas the lower ones were obtained for the Mulliken atomic charges. It means that atomic charges calculated in APT method better reflect the experimentally obtained information about electronic charge density that Mulliken method.

Table 6
Theoretical chemical shifts for *p*-coumarates in ^{1}H and ^{13}C NMR spectra, δ (ppm); atom numbering in Fig. 1

	p-Coumaric acid	Li *p*-coumarate	Na *p*-coumarate	K *p*-coumarate
Proton number				
1	6.03	–	–	–
2	8.10	8.10	8.09	8.06
3	6.97	6.85	6.82	6.80
4	3.56	3.32	3.27	3.17
5	7.06	6.94	6.90	6.84
6	7.65	7.57	7.56	7.54
7	6.44	6.31	6.30	6.26
8	8.15	8.46	8.47	8.41
Carbon number				
1	138.65	141.52	141.88	142.76
2	133.53	132.84	132.51	132.03
3	126.61	125.83	125.73	127.25
4	171.50	169.16	168.95	168.18
5	125.29	124.36	124.22	123.90
6	143.21	141.33	140.99	140.37
7	180.18	194.03	193.85	195.64
8	120.09	125.53	125.68	127.25
9	156.33	154.50	154.46	152.70
Oxygen number				
1	203.71	307.85	310.05	360.90
2	458.85	402.60	398.15	391.45
3	118.26	112.49	111.37	109.48

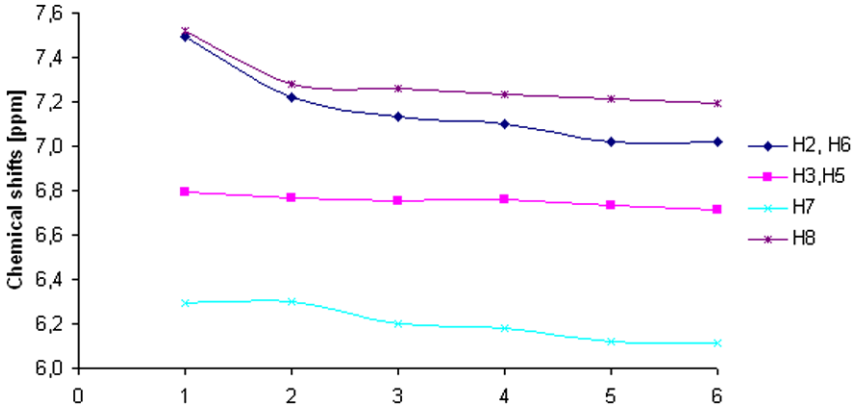

Fig. 4. Experimental chemical shifts of protons from ^{1}H NMR spectra of alkali metal *p*-coumarates in comparison with *p*-coumaric acid. (Colors are visible in the online version of the article; http://dx.doi.org/10.3233/SPE-2012-0568.)

4. Conclusions

Spectral characteristic of the alkali metal *p*-coumarates has been done. Replacement of carboxylic group hydrogen with alkali metal ions brought about some characteristic changes in molecular spectra

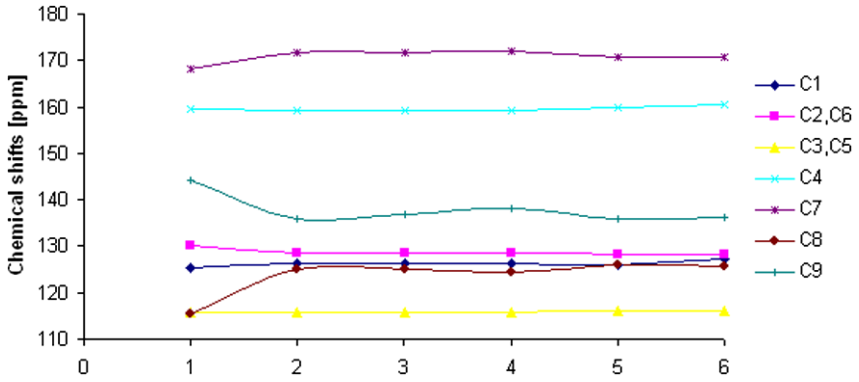

Fig. 5. Experimental chemical shifts of carbons from ^{13}C NMR spectra of alkali metal *p*-coumarates in comparison with *p*-coumaric acid. (Colors are visible in the online version of the article; http://dx.doi.org/10.3233/SPE-2012-0568.)

as well as in geometrical structure of studied molecules. The decrease in chemical shifts of almost all protons from ^{1}H NMR spectra of *p*-coumarates was observed in comparison with the spectra of *p*-coumaric acid. It points at a decrease in ring current intensity in *p*-coumarates in comparison with acid molecule. The highest correlation coefficients were obtained for experimental and theoretical data calculated by the APT method. Good agreement was obtained between the experimental and calculated infrared spectra. The intensities and wavenumber of the majority of aromatic system bands in IR and Raman spectra increased in the case of salts comparing to the free ligand. The magnitudes of separation between wavenumbers of asymmetrical and symmetrical stretching vibrations of carboxylic group $\Delta\nu$ increase in the series Na < K < Rb < Cs *p*-coumarates. It indicates the increase in degree of ionic bonding between metal ion and COO^{-} group in the mentioned series. The values of Aj and HOMA aromaticity indices are almost the same in the series: acid → Li → Na → K salts. Little differences are observed for BAC. This suggests that studied compound posses similar aromatic properties.

Acknowledgement

This work was supported by Polish Ministry of Science and Higher Education in the frame of Grant No. N N317 111838.

References

[1] T. Biswick, D.-H. Park, Y.-G. Shul and J.-H. Choy, *J. Phys. Chem. Solids* **71** (2010), 647–649.
[2] M.H. Borawska, P. Koczoń, J. Piekut, R. Świsłocka and W. Lewandowski, *J. Mol. Struct.* **919** (2009), 284–289.
[3] R.F. Bryan and P.G. Forcier, *Mol. Cryst. Liq. Cryst.* **60** (1980), 157–166.
[4] M.J. Frisch, G.W. Trucks, H.B. Schlegel, G.E. Scuseria, M.A. Robb, J.R. Cheeseman, V.G. Zakrzewski, J.A. Montgomery Jr., R.E. Stratmann, J.C. Burant, S. Dapprich, J.M. Millam, A.D. Daniels, K.N. Kudin, M.C. Strain, O. Farkas, J. Tomasi, V. Barone, M. Cossi, R. Cammi, B. Mennucci, C. Pomelli, C. Adamo, S. CliVord, J. Ochterski, G.A. Petersson, P.Y. Ayala, Q. Cui, K. Morokuma, N. Rega, P. Salvador, J.J. Dannenberg, D.K. Malick, A.D. Rabuck, K. Raghavachari, J.B. Foresman, J. Cioslowski, J.V. Ortiz, A.G. Baboul, B.B. Stefanov, G. Liu, A. Liashenko, P. Piskorz, I. Komaromi, R. Gomperts, R.L. Martin, D.J. Fox, T. Keith, M.A. Al-Laham, C.Y. Peng, A. Nanayakkara, M. Challacombe, P.M.W. Gill, B. Johnson, W. Chen, M.W. Wong, J.L. Andres, C. Gonzalez, M. Head-Gordon, E.S. Replogle and J.A. Pople, *Gaussian 98*, Revision A.11.2, Pittsburgh, PA, 2001.
[5] F. Herrera, C. Pulgarin, V. Nadtochenko and J. Kiwi, *Appl. Catal. B: Environ.* **17** (1998), 141–156.
[6] M. Kalinowska, R. Świsłocka and W. Lewandowski, *J. Mol. Struct.* **834–836** (2007), 572–580.

[7] T.M. Krygowski and M. Cyrański, *Tetrahedron* **52** (1996), 1713–1722.
[8] W. Lewandowski, M. Kalinowska and H. Lewandowska, *J. Inorg. Biochem.* **99** (2005), 1407–1423.
[9] K. Liu, L. Yan, G. Yao and X. Guo, *J. Chromatogr. B* **831** (2006), 303–306.
[10] M. Putschoögl, P. Zirak and A. Penzkofer, *Chem. Phys.* **343** (2008), 107–120.
[11] D. Salameh, C. Brandam, W. Medawar, R. Lteif and P. Strehaiano, *Food Chem.* **107** (2008), 1661–1667.
[12] M. Samsonowicz, R. Świsłocka, E. Regulska and W. Lewandowski, *J. Mol. Struct.* **887** (2008), 220–228.
[13] S. Sebastian, N. Sundaraganesan and S. Manoharan, *Spectrochim. Acta A* **74** (2009), 312–323.
[14] G. Świderski, M. Kalinowska, S. Wojtulewski and W. Lewandowski, *Spectrochim. Acta A* **64** (2006), 24–33.
[15] H. Utsumi, K. Fujii, H. Irie, A. Furusaki and I. Nitta, *J. Chem. Soc. Jpn. Pure Chem.* **91** (1970), 928.
[16] G. Varsányi, *Assignments for Vibrational Spectra of 700 Benzene Derivatives*, Akademia Kiado, Budapest, 1973.